

# Modeling the effects of p-modulation doping in InAs quantum dot devices

Benjamin Maglio  
School of Physics &  
Astronomy  
Cardiff University  
Cardiff, United Kingdom  
MaglioB2@Cardiff.ac.uk

Lydia Jarvis  
School of Physics &  
Astronomy  
Cardiff University  
Cardiff, United Kingdom  
JarvisLK@Cardiff.ac.uk

Mingchu Tang  
Department of Electronic and  
Electrical Engineering  
University College London  
London, United Kingdom  
Mingchu.Tang.11@UCL.ac.uk

Huiyun Liu  
Department of Electronic and  
Electrical Engineering  
University College London  
London, United Kingdom  
Huiyun.Liu@UCL.ac.uk

Peter M. Smowton  
School of Physics & Astronomy  
Cardiff University  
Cardiff, United Kingdom  
SmowtonPM@Cardiff.ac.uk

**Abstract**—a modeling routine has been developed to quantify the effects of p-modulation doping in the waveguide core region of InAs quantum dot (QD) devices. Utilizing one dimensional approximations, simulated outputs of reverse and forward devices are simulated providing insight into absorption and gain properties.

## I. INTRODUCTION

Quantum dot (QD) based optoelectronics have been much discussed for over 20 years due to improvements over quantum wells (QWs) for application to photonic integrated circuits (PICs)<sup>[1]</sup>. Upscaling PIC manufacture by growing III-V alloys on Silicon substrates provides a pathway to mass producing low cost PICs, provided further challenges may be overcome<sup>[2]</sup>.

A consequence of growing III-V alloys directly on Silicon is the formation of threading dislocations (TDs), resulting from the difference in lattice parameters. QDs provide a high tolerance to TDs<sup>[1]</sup> compared to QWs, while still providing high performance at telecom wavelengths. Nevertheless, due to a sizeable difference between electron and hole effective masses, there is an imbalance in carrier occupation. In QWs this is corrected by introducing compressively strained layers<sup>[1],[3]</sup>, whereas for QDs this is not viable due to strain being an integral part of growth.

One solution is p-modulation doping in the barriers near the QD layers, providing a reservoir of holes for the highest valence band states. Benefits of this technique are numerous with evidence suggesting increased modal gain<sup>[3]</sup>, radiative recombination<sup>[4]</sup>, and reduced threshold current density<sup>[5]</sup>. Undeniably, there are disadvantages including higher nonradiative recombination<sup>[3]</sup> and carrier induced index changes<sup>[6]</sup>. Correct integration may still provide benefits, improving performance of QDs grown on Silicon, paving the way for convincing, large scale, photonic integration.

Gain in p-doped InAs QDs has been investigated thoroughly both theoretically<sup>[1],[2],[4],[5]</sup> and experimentally<sup>[2],[3],[5],[7]</sup>. Theoretically, modeling is intricate, even prior to the added complexity of p-doping. More so, the growth of QDs can deviate from prediction, remaining difficult to decouple the effects of different doping parameters from natural variations in growth (like size distributions, or index changes)<sup>[6],[8]</sup>.

In this work, we present a semi-empirical model, influenced by measurable parameters, with one dimensional approximations. Particular attention is given to analysis of absorption, though gain is also reported, providing insight into the properties of QD devices such as modulators and lasers, essential components in serious PIC platforms.

## II. MODELING PROCEDURE

The routine developed combines, bandstructure calculations via a self-consistent Schrödinger-Poisson-current continuity solver from Nextano<sup>[9]</sup>, calculation of the optical confinement factor in Lumerical's MODE waveguide simulator, followed by an in-house program for calculation of modal absorption and gain. Only layer thicknesses are defined, simplifying the model and eliminating the complexity associated with multi-dimensional QD simulations. However, as subsequently described, further approximations are necessary to maintain realistic outputs.

Opposed to abrupt material changes, as in QWs, parabolic wells are used for the  $\text{In}_x\text{Ga}_{1-x}\text{As}$  QDs with  $x=0.16$ -1.0 between QD edge and center. Thus, the electronic states are almost equally spaced with half integer values of  $\hbar\omega$  providing good agreement with measurement. As in [5], the strain distributions in the QDs are assumed uniform, so an added correction, here to the bandgap, provides equivalence to corresponding measurements. Significant discrepancy arises between the density of states (DOS) functions for QWs and QDs, modeled as Heavy-side step and delta functions respectively. Here, a mass tensor ellipsoid is employed to solve this issue, with transverse masses reduced to equate the effective DOS to the dot density.

Next, the outputs are read through the in-house program

P-type GaAs – AlGaAs Cladding	≈1700nm	x 7
GaAs Barrier	42.5nm	
$\text{In}_{0.16}\text{Ga}_{0.84}\text{As}$ Capping layer	5nm	
InAs Dot Layer ( $5 \times 10^{10}\text{cm}^{-3}$ )	3ML	
$\text{In}_{0.16}\text{Ga}_{0.84}\text{As}$ Wetting layer	2nm	
GaAs Confinement Layer	42.5nm	
N-type GaAs – AlGaAs Cladding	≈1700nm	

Fig. 1. 1.31 $\mu\text{m}$  InAs QD epistructure grown on GaAs substrate. P-doping is incorporated within GaAs barrier region.

calculating modal absorption,  $\alpha$  (or gain,  $g$ ) similarly to [4].

$$\alpha = \sum_l \sum_{c,v} \frac{\Gamma_l \pi e^2 \hbar |M_b|^2 N_d s_i}{cm_0 \epsilon_0 n_r L_z E_{cv}} S(E_{cv}) G(E_{cv}) (f_v - f_c) \quad (1)$$

Here, each transition between  $c$ ,  $v$ , conduction and valence band states, are summed followed by contributions per layer,  $l$ . This allows for a layer-by-layer analysis additionally to the full device. Elementary charge,  $e$ , Dirac constant,  $\hbar$ , speed of light in a vacuum,  $c$ , electron rest mass,  $m_0$  and vacuum permittivity,  $\epsilon_0$  are used.  $\Gamma_l$  is the optical confinement per layer,  $N_d$  the dot density,  $n_r$  the real refractive index,  $L_z$  the dot height,  $E_{cv}$  the transition energy, and  $s_i$  the degeneracy.  $|M_b|^2$  is the bulk matrix element containing Kane parameter. Homogeneous and inhomogeneous broadening are represented as hyperbolic secant function,  $S(E_{cv})$ , and Gaussian function,  $G(E_{cv})$ , respectively. Finally, equation (1) is multiplied at each layer by the occupation difference,  $(f_v - f_c)$ , from Fermi-Dirac statistics with corresponding conduction, valence, and quasi Fermi-level energies. The wavefunction overlap is omitted as the approximation does not fully account for the confinement of the QD, following [5].

### III. RESULTS

Figure 2 demonstrates clear distortion in the p-doped bandstructure, increasing with reverse bias. A clear carrier-blocking, state-filling effect is apparent for reverse and forward bias respectively, from the positions of the quasi Fermi-levels, reducing absorption and increasing gain. Additionally, a variation in the transition energy observed with increasing reverse bias, provides additional broadening. These effects are apparent in the absorption spectrum in figure 3, though when isolated we observe the most significant increase in the homogeneous broadening is dependent upon carrier scattering, with a reduction of  $\approx 20$ fs between scattering events, found from fitted absorption spectra in doped samples.

When pumped, state-filling increases differential gain and reduces threshold current density, though increased carrier scattering impairs the gain at higher current densities. Beneficially for modulator operation, it is expected that a large reduction in insertion loss (IL) can be accounted for by the increased carrier scattering rate. This is detrimental to laser performance and expected to be an underestimate, increasing up to eight times with carrier injection in [2]. Though some change in broadening with temperature, it is expected a combination of remote ionized impurity and carrier-carrier scattering contribute, though a more sophisticated model, with many-body effects must be utilized to decouple the dominant mechanism. Quenched absorption signifies reduced extinction ratio (ER), though an increased

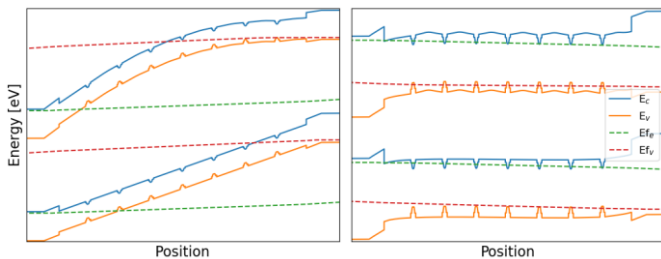


Fig. 2. P-doped (upper), undoped (lower) bandstructures at reverse (left) and forward (right) bias. 10nm thick,  $5 \times 10^{17} \text{cm}^{-3}$  doped layer at 15nm above dot layers. Data offset to provide comparison.

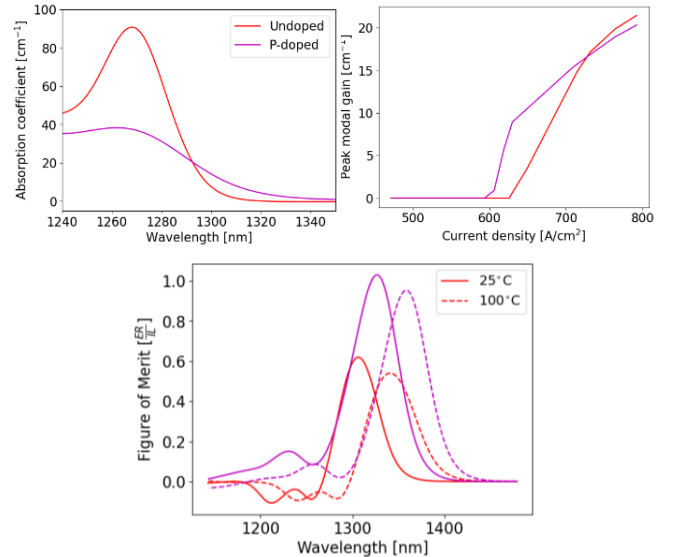


Fig. 3. Absorption (left) and peak modal gain (right) with FoM (lower), for undoped and p-doped structures. Only ground state contributions considered and a 4V swing in reverse bias used to calculate FoM.

figure of merit (FoM), or ER: IL, is calculated, with stability between 25-100°C, indicating good modulator performance.

### IV. SUMMARY

A routine has been developed to quantify the effects of p-doped InAs QD devices. Analysis shows significant benefits from state-filling, though increased carrier scattering has both positive and negative implications for the design of modulators and lasers respectively.

### REFERENCES

- [1] M. Saldutti, A. Tibaldi, F. Cappelluti, and M. Gioannini, "Impact of carrier transport on the performance of QD lasers on silicon: a drift-diffusion approach," *Photonics Res.*, vol. 8, no. 8, p. 1388, Aug. 2020, doi: 10.1364/PRJ.394076.
- [2] Z. Zhang, D. Jung, J. C. Norman, P. Patel, W. W. Chow, and J. E. Bowers, "Effects of modulation  $p$  doping in InAs quantum dot lasers on silicon," *Appl. Phys. Lett.*, vol. 113, no. 6, p. 061105, Aug. 2018, doi: 10.1063/1.5040792.
- [3] P. M. Smowton, I. C. Sandall, H. Y. Liu, and M. Hopkinson, "Gain in p-doped quantum dot lasers," *J. Appl. Phys.*, vol. 101, no. 1, p. 013107, Jan. 2007, doi: 10.1063/1.2405738.
- [4] A. A. Dikshit and J. M. Pikal, "Carrier Distribution, Gain, and Lasing in 1.3micron InAs-InGaAs Quantum-Dot Lasers," *IEEE J. Quantum Electron.*, vol. 40, no. 2, pp. 105–112, Feb. 2004, doi: 10.1109/JQE.2003.821532.
- [5] J. Kim and S. L. Chuang, "Theoretical and Experimental Study of Optical Gain, Refractive Index Change, and Linewidth Enhancement Factor of p-Doped Quantum-Dot Lasers," *IEEE J. Quantum Electron.*, vol. 42, no. 9, pp. 942–952, Sep. 2006, doi: 10.1109/JQE.2006.880380.
- [6] J. C. Norman *et al.*, "A Review of High-Performance Quantum Dot Lasers on Silicon," *IEEE J. Quantum Electron.*, vol. 55, no. 2, pp. 1–11, Apr. 2019, doi: 10.1109/JQE.2019.2901508.
- [7] I. C. Sandall *et al.*, "The effect of  $p$  doping in InAs quantum dot lasers," *Appl. Phys. Lett.*, vol. 88, no. 11, p. 111113, Mar. 2006, doi: 10.1063/1.2186078.
- [8] I. O'Driscoll, P. M. Smowton, and P. Blood, "Low-Temperature Nonthermal Population of InAs-GaAs Quantum Dots," *IEEE J. Quantum Electron.*, vol. 45, no. 4, pp. 380–387, Apr. 2009, doi: 10.1109/JQE.2009.2013869.
- [9] S. Birner *et al.*, "nextnano: General Purpose 3-D Simulations," *IEEE Trans. Electron Devices*, vol. 54, no. 9, pp. 2137–2142, Sep. 2007, doi: 10.1109/TED.2007.902871.